B20099

Flanagan, K. J.; Ryan, A. A.; Twamley, B.; Senge, M. O. (2020):
Influence of meso-linker attachment on the formation of core···π interactions in urea-functionalized porphyrins.
Zeitschrift für Naturforschung 75b, 755–764. doi: 10.1515/znb-2020-0099

Keith J. Flanagan, Aoife A. Ryan, Brendan Twamley, and Mathias O. Senge*

Influence of meso-linker attachment on the formation of core···π interactions in urea-functionalized porphyrins

https://doi.org/10.1515/znb-2020-0099

Received June 5, 2020; accepted July 10, 2020

*** Corresponding author: Prof. Dr. Mathias O. Senge,** School of Chemistry, Trinity Biomedical Sciences Institute, 152–160 Pearse Street, Trinity College Dublin, The University of Dublin, Dublin 2, Ireland; FAX: 00353-1-896-8536, e-mail: sengem@tcd.ie

Keith J. Flanagan, Aoife A. Ryan: School of Chemistry, Trinity Biomedical Sciences Institute, 152–160 Pearse Street, Trinity College Dublin, The University of Dublin, Dublin 2, Ireland.

Brendan Twamley: School of Chemistry, Trinity College Dublin, The University of Dublin, Dublin 2, Ireland

Abstract: The ability to cover the face of a porphyrin macrocycle selectively is an attractive feature for concepts such as catalysis and anion binding that are reliant on porphyrin core interactions. Herein, we have synthesized a family of mono-urea functionalized porphyrin complexes with intent to investigate their potential to form core···π interactions selectively to one face of the porphyrin macrocycle. By altering the distance between the urea moiety and the porphyrin through direct linkage or introducing a linker group we can control the formation of the core interactions. This is clearly seen in the crystal structure of 1-phenyl-3-(2-([10,15,20-

triphenylporphyrinato]zinc(II)-5-yl)phenyl)urea where a unique face capping effect is demonstrated. In the crystal of this complex, there is a hydrogen-bonding network between the urea group and the axial methanol ligand forming head-to-tail aggregates with the Zn–O axis all molecules pointing in one direction.

Keywords: porphyrins; urea formation; crystal structure; Suzuki reaction; Sonogashira reaction

Introduction

Urea-based porphyrins have been used over the past decades in fields such as biomimetic multipoint hydrogen-bonding [1], as receptors for simple sugars [2], growing thin-layer films [3], or in the form of picket fence porphyrins in anion binding [4]. We recently showed how a 2,3,7,8,12,13,17,18-octaethyl-5,10,15,20-tetrakis(2-aminophenyl)porphyrin in which the four 2-aminophenyl moieties point towards one face of the porphyrin macrocycle (α_4 atropisomer) can be used as a sensor [5]. In this case, the porphyrin can bind a phosphoric or sulfonic moiety in a face-selective 'lock and key' mode through the amino group, which is reliant on the isomer formation of the porphyrin. This indicates that having a selective approach to modify the 'face' of the porphyrin macrocycle can be important when considering concepts such as catalytic reactions that are reliant on core porphyrin reactions or anion binding [6–8]. Possible approaches are 'strapping' of porphyrins [9], the use of superstructured and/or unique atropisomeric complexes [6], or incorporation of a suitable substituent. The latter is exemplified in the enantioselective photo- and transition metal catalysts developed by the Bach group [10, 11].

With this in mind, we considered the potential of having a method of covering one face of a porphyrin macrocycle in a controllable manner without incurring conformation constraints using linker groups that potentially can be used for hydrogen bonding. Herein we report on an

exploratory synthesis of urea-functionalized porphyrin molecules that are either directly-linked or contain a spacer unit (Figure 1) and describe how the orientation of the arm is affected by the distance between the urea moiety and the porphyrin macrocycle.

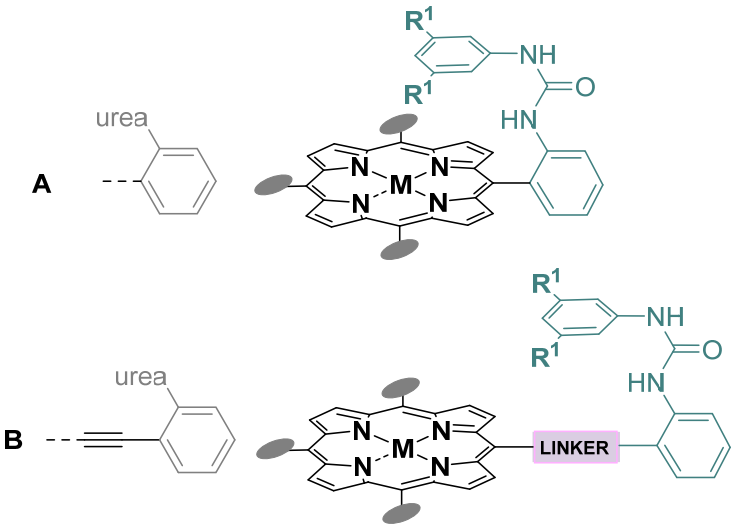

Figure 1: Target systems.

Results and Discussion

Synthesis

The synthesis of urea porphyrins involved two desired targets, direct meso attachment and the use of a linker to increase the distance between the central and peripheral units (Figure 1). The first attempt of this process was to form a direct linkage between a borylated porphyrin **1** and a brominated urea complex **2** through a Suzuki coupling process to generate Target A (Scheme 1). A few different conditions were trialed; however, ultimately we adopted the well-known procedure developed by Therien and co-workers [12]. The main drawback of this strategy is that an excess of porphyrin is required for optimal synthesis. Inevitably, due to this excess, the main products of the reaction are the deborylated porphyrin and the homo-coupled meso-meso directly-linked porphyrin dimer. The target was synthesized, albeit in a low yield of less than 30%, based on 1 equivalent of urea (10 mg). When this reaction was scaled up, the overall

yields dramatically decreased. In essence, this is not an ideal strategy as the more expensive porphyrin starting material is consumed in large amounts and the side products are not re-usable, i. e. no starting porphyrin material is recovered. Thus, new strategies to overcome these issues were investigated.

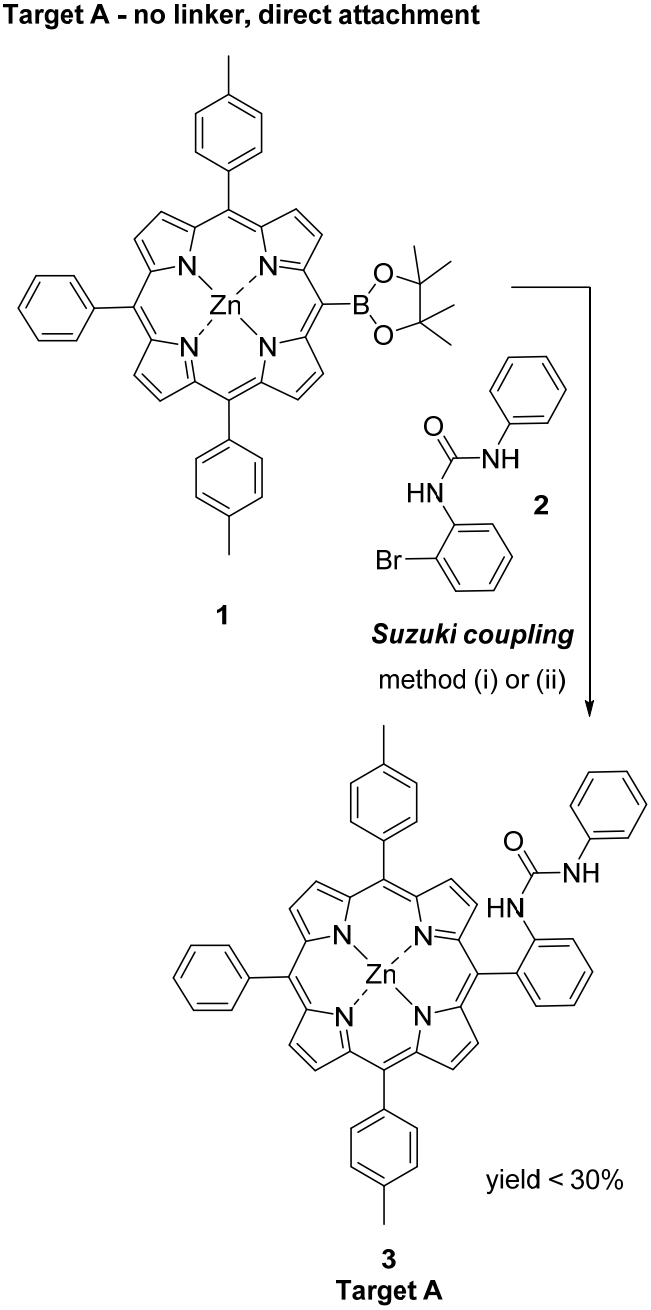

Scheme 1: Suzuki coupling. Reagents and Conditions: Porphyrin (2–3 eq.), urea (1 eq.), $Ba(OH)_2 \cdot 8H_2O$ (4 eq.), $Pd(PPh_3)_4$ (5%). (i) solvent = DME-H_2O at 80 °C; (ii) solvent = THF-H_2O at 60 °C.

By pre-functionalizing the porphyrin unit with an anilinyl moiety it was assumed that the further functionalization of this moiety could be used to achieve the desired urea compound in much higher yields. 2-Bromoaniline **4** was borylated to achieve compound **5** in a process similar to that reported by Yan *et al.* [13]. These compounds could then be used without further purification in a Suzuki coupling reaction with an appropriate meso-brominated porphyrin to give the desired aniline substituted porphyrins **6a**–**6c** in high yields (Scheme 2). Following this, the urea forming reaction could be carried out at room temperature by stirring porphyrin **6** with an isocyanate for 2–24 hours yielding the desired urea porphyrin (Target A) in >70% yield.

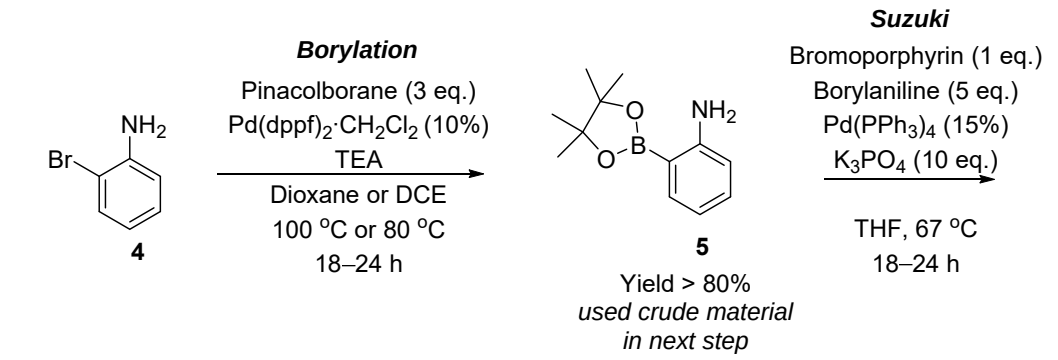

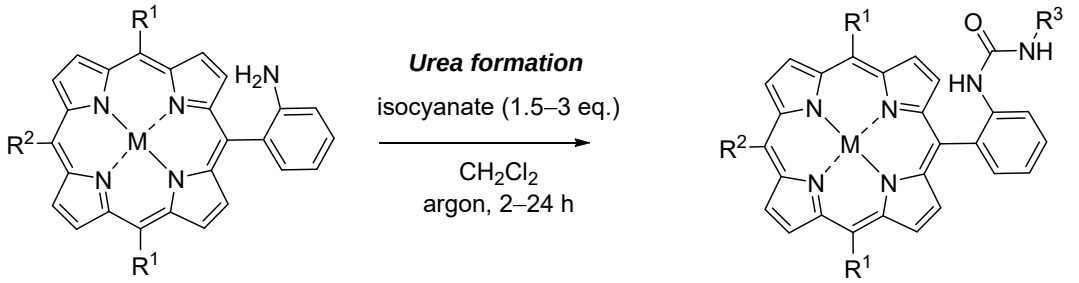

6a: R^1 = Ph, R^2 = H, M = 2H
6b: R^1 = R^2 = Ph, M = 2H
6c: R^1 = R^2 = Ph, M = Zn(II)

Yields >80%

7a: R^1 = Ph, R^2 = H, R^3 = bis(trifluoromethyl)phenyl, M = 2H (i)
7b: R^1 = Ph, R^2 = H, R^3 = bis(trifluoromethyl)phenyl, M = Zn(II)
7c: R^1 = R^2 = R^3 = Ph, M = 2H (i)
7d: R^1 = R^2 = R^3 = Ph, M = Zn(II)
7e: R^1 = R^2 = Ph, R^3 = bis(trifluoromethyl)phenyl, M = Zn(II)

Scheme 2: Synthesis of a directly meso-linked urea porphyrin. (i) $Zn(OAc)_2 \cdot 2H_2O$, $CHCl_3$-MeOH.

Concurrently, the investigation into the acetylene-linked system (Target B) was carried out. The Sonogashira coupling of an alkynyl porphyrin [5-ethinyl-10,20-bis(2-methylphenyl)-15-phenylporphyrin] and the bromo-urea **2** was carried out. However, in contrast to the Suzuki coupling shown in Scheme 1, no porphyrin was isolated *via* any of the conditions investigated. The predominant product in all cases was the homo-coupled butadiyne-linked porphyrin dimer. As above, functionalizing the porphyrin prior to urea formation was considered to be a much more viable alternative. Compound **4** was functionalized with an acetylene moiety using a method similar to that reported by Abraham *et al*. [14] and then attached to a porphyrin macrocycle through a Sonogashira coupling reaction to give porphyrin **10** (Scheme 3). This was followed by urea formation at room temperature by stirring porphyrin **10** with an isocyanate for 2 hours yielding the desired urea porphyrin (Target B) in >70% yields.

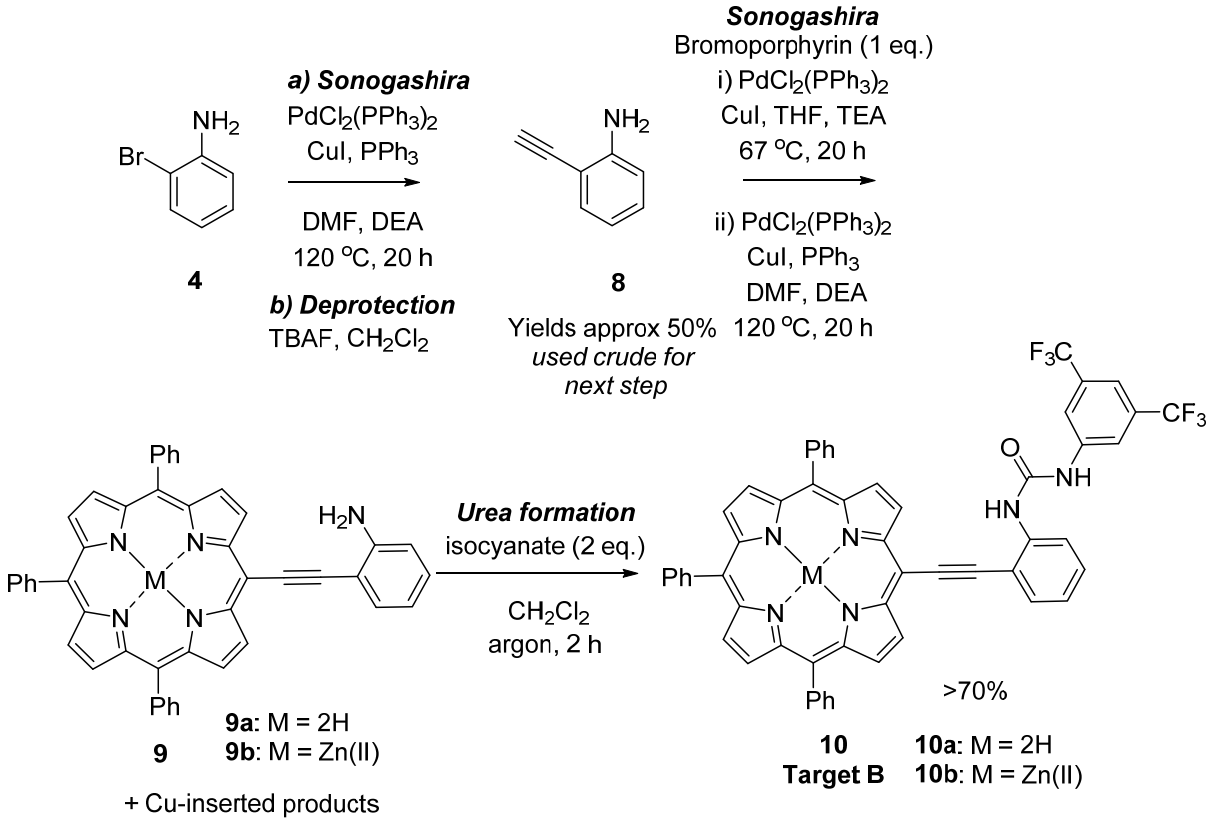

Scheme 3: Synthesis of the acetylene-linked urea porphyrin. (i) $Zn(OAc)_2 \cdot 2H_2O$, $CHCl_3$-MeOH.

X-ray crystallography

The crystal structure of **7d·MeOH** was determined by X-ray crystallography after the recrystallization of **7d** *via* slow diffusion technique (CH_2Cl_2/MeOH). In this structure, it can be clearly seen that the phenyl moiety of the meso urea group is held directly over the porphyrin macrocycle plane (Figure 2) at a distance of 2.730(9) Å. This feature is quite interesting as the urea group is essentially acting as a block to this face of the porphyrin. In comparison to other urea porphyrin crystal structures, this mode of action is quite unique. In the CCDC database [15], there are only examples of tetrasubstituted urea porphyrins and in none of them do the phenyl moieties interact with the face of the porphyrin macrocycle as is the case with **7d·MeOH** [15–17]. This can be graphically explained by looking at the Hirshfeld surface [18] of **7d·MeOH** (Figure 3), which shows that the phenyl moiety takes up a large portion of the surface area on the face of the porphyrin [19]. The urea meso-substituent is held at 91.9(2)° in regards to the 24-atom mean plane of the porphyrin macrocycle. The other three phenyl substituents are more tilted into the plane with angles of 66.2(3), 75.0(2), and 61.6(3)° (C10, C15, and C20, respectively). This is a result of the π interaction between the urea phenyl moiety and the porphyrin macrocycle rotating the urea phenyl group to an orthogonal orientation. In the packing of this structure, there is one key feature which is the hydrogen-bonded network between the hydrogen atom on the axial methanol ligand (H1S) and the oxygen atom of the urea moiety (O1) (O1S–H1S···O1, 1.846(6) Å and 161.3(5)°) (Figure 4). This linear network organizes the porphyrin units in a head-to-tail sequence with all MeOH units pointing above the plane and all urea units pointing below the plane. A second short contact is seen between the C12 of the macrocycle ring and O1 of the urea moiety (C12–H12···O1, 2.675(1) Å and

155.3(1)°) (Figure 5). This creates a staggered packing pattern in the unit cell with the Zn–O axes of the porphyrin units all pointing in the same direction.

While we were not able to obtain a crystal structure of Target B, there are some predictions we can make at this point. Due to the extra separation that would be imparted by the acetylene linker (~2.6 Å, based on the average bond length recorded in the CCDC [15]), the distance between the phenyl moiety and the porphyrin would be too great establish a significant interaction. Therefore, we can rule out any ability for Target B to cap the face of the porphyrin. A direct link to the porphyrin macrocycle (Target A) is essential in this case; however, this problem could potentially be circumvented by altering the urea functionality to include a longer chain motif. This could be an area of further research, but as pointed out by Burg *et al.*, increased bulk decreases the overall conversion in any catalytic system [11].

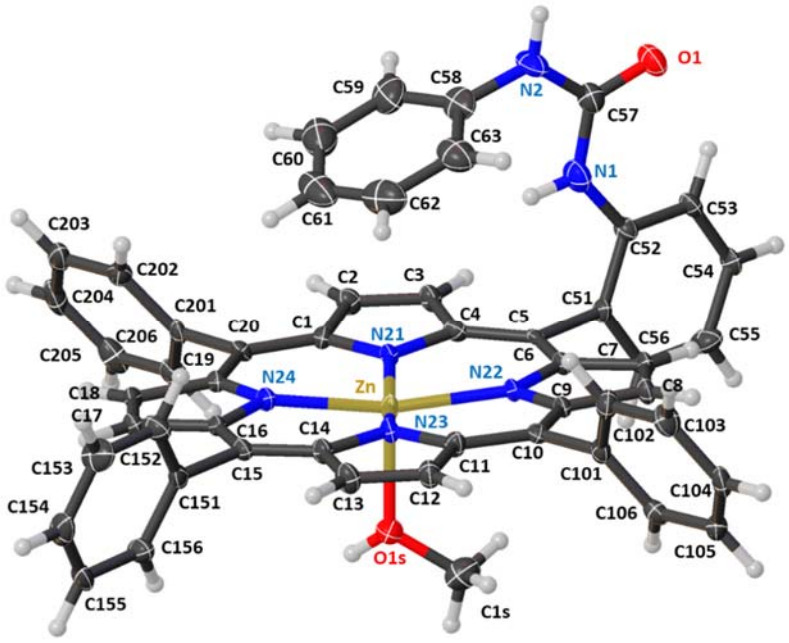

Figure 2: Molecular structure of **7d·MeOH** in the crystal (solvent CH_2Cl_2 molecules have been omitted for clarity). Displacement ellipsoids are shown at the 50% probability level.

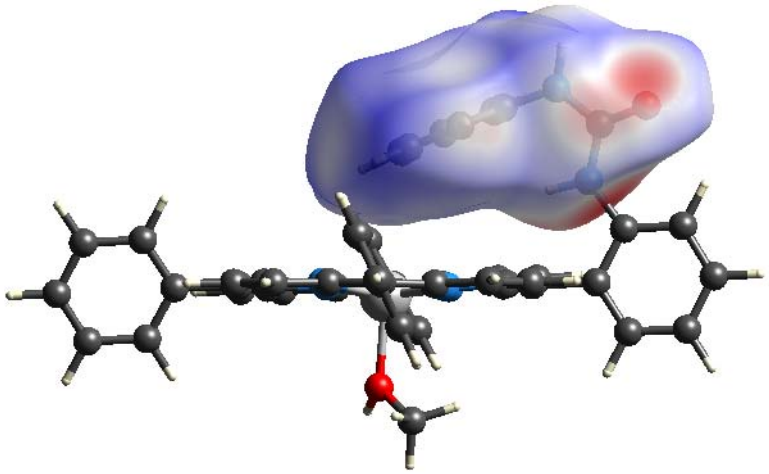

Figure 3: Hirshfeld surface analysis showing the space occupied by the phenyl moiety in crystalline **7d·MeOH**.

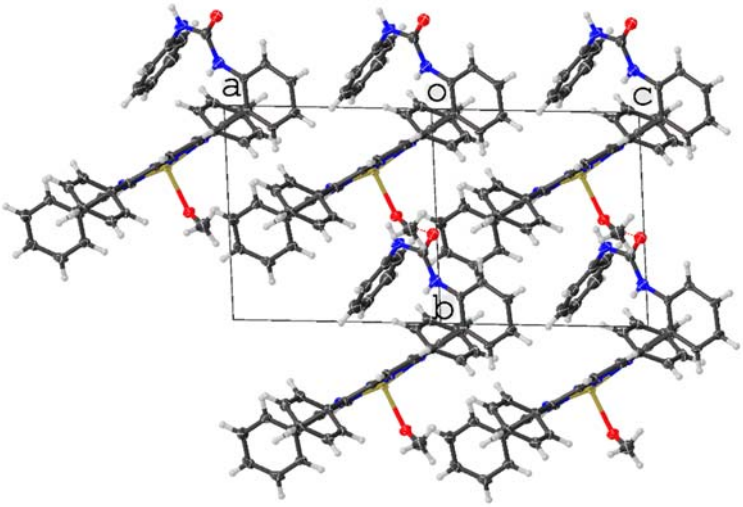

Figure 4: Packing in the crystal of **7d·MeOH** viewed down the 111 plane (solvate CH_2Cl_2 molecules have been omitted for clarity). Displacement ellipsoids are shown at the 50% probability level.

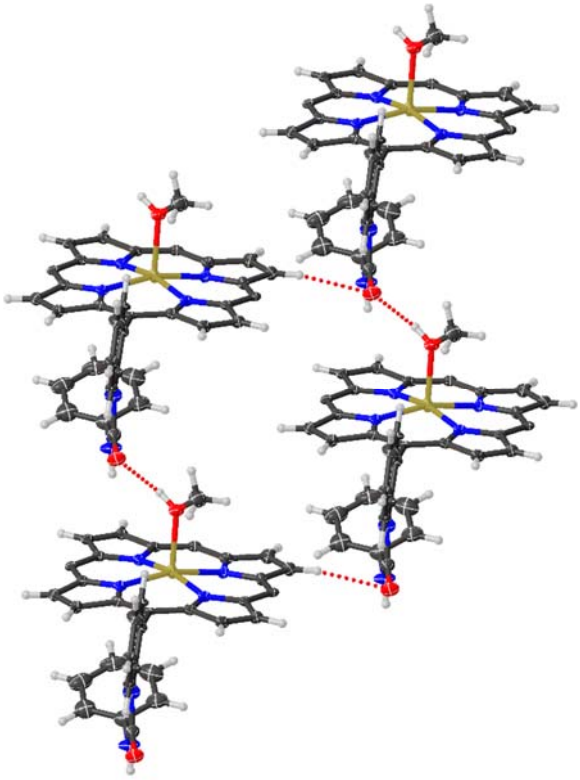

Figure 5: Section of the crystal structure of **7d·MeOH** showing the extended hydrogen-bonding network and the short contacts between individual molecules. Solvate molecules and meso-phenyl substituents have been omitted for clarity. Displacement ellipsoids are shown at the 50% probability level.

Conclusion

We have synthesized three new mono-aniline based porphyrins and seven new mono-urea porphyrins through Suzuki (Target A) and Sonogashira (Target B) coupling reactions. From this series, we were able to determine by single-crystal X-ray diffraction the structure of **7d·MeOH** which showed a unique face interaction between the urea phenyl moiety and the porphyrin macrocycle. This has the effect of capping the face of the porphyrin macrocycle, preventing any other interaction with one side of the face of the porphyrin macrocycle. In this case, there is a reliance on the distance between the porphyrin macrocycle and urea functionality. Within the crystal, there is a hydrogen-bonding network between the urea group

and the axial methanol ligand which leads to a head-to-tail aggregation with the Zn–O axes pointing in the same direction.

Experimental Section

General

General experimental conditions for the synthesis and characterization of the compounds were as described before [20]. The characterization of **6b** and **6c** has been previously reported [21, 22]. All materials were of analytical or reagent grade and used as received without further purification.

*5-(2-Aminophenyl)-10,20-diphenylporphyrin (**6a**)*

5-Bromo-10,20-diphenylporphyrin (210 mg, 0.388 mmol) was dried under vacuum for 20 min in a 100 mL Schlenk tube. Anhydrous THF (15 mL) was added to dissolve the porphyrin and the solution was degassed *via* 3 freeze-pump-thaw cycles. K_3PO_4 (822 mg, 3.88 mmol,), $Pd(PPh_3)_4$ (68 mg, 0.058 mmol) and 2-(4,4,5,5-tetramethyl-1,3,2-dioxaborolan-2-yl)aniline (0.4 M in anhydrous THF, 4.84 mL, 1.939 mmol) were added and the reaction vessel was heated to 67 °C and left to stir at this temperature for 18 h. Upon complete consumption of the starting material, the solvent was removed *in vacuo* and the residue was redissolved in CH_2Cl_2. This solution was washed with sat. aqueous $NaHCO_3$ solution, water and brine, and the organic extracts were dried over Na_2SO_4 and filtered, and the solvents were removed *in vacuo*. The purple residue was triturated with MeOH and filtered using a Buchner apparatus to yield a purple solid (170 mg, 0.307 mmol, 79%). M. p. = 275–276 °C. – R_f (CH_2Cl_2-hexanes 1 : 1, *v*/*v* + 1% MeOH) = 0.62. – ^{1}H NMR (400 MHz, $CDCl_3$): δ = –2.97 (s, 2H, porphyrin-N*H*), 3.50 (s, 2H, NH_2), 7.09 (d, *J* = 7.8 Hz, 1H, aryl-*H*), 7.16 (t, *J* = 7.4 Hz, aryl-*H*), 7.59 (t, *J* = 7.4 Hz, aryl-*H*), 7.75–7.80 (m, 6H, Ph-*H*), 7.87 (d, *J* = 7.4 Hz, 1H, aryl-*H*), 8.23 (m, 4H, Ph-*H*), 8.89–8.95

(m, 4H, *β-H*), 9.00 (d, *J* = 4.1 Hz, 2H, *β-H*), 9.32 (d, *J* = 4.1 Hz, 2H, *β-H*), 10.22 ppm (s, 1H, meso-*H*). – ^{13}C NMR (100 MHz, $CDCl_3$): δ = 105.2, 115.2, 115.9, 117.4, 119.5, 126.8, 127.6, 127.7, 129.6, 131.0, 131.4, 134.7, 134.8, 141.6, 146.9 ppm. – UV/Vis (CH_2Cl_2): λ_{max} (lg ε) = 412 (5.29), 508 (4.04), 544 (3.51), 582 (3.59), 638 nm (3.25). – HRMS (MALDI): *m*/*z* = 553.2268 (calcd. 553.2266 for $C_{38}H_{27}N_5$).

*1-(3,5-Bis(trifluoromethyl)phenyl)-3-(2-(5,15-diphenylporphyrin-10-yl)phenyl)urea (**7a**)*

5-(2-Aminophenyl)-10,20-diphenylporphyrin (130 mg, 0.235 mmol) was dried under vacuum for 10 min in a 100 mL Schlenk flask. Anhydrous CH_2Cl_2 (10 mL) was added to dissolve the porphyrin. 3,5-Bistrifluoromethylphenyl isocyanate (60 μL, 0.352 mmol) was added and the solution was left to stir at room temperature for 18 h. TLC analysis (CH_2Cl_2-hexane 1 : 1, *v*/*v* + 2% MeOH) showed the presence of starting material, hence more isocyanate (40 μL, 0.235 mmol) was added. After a further reaction time of 2 h, the reaction was complete and the solvent was removed *in vacuo*. The residue was redissolved in CH_2Cl_2 and the solution filtered through a short plug of silica using CH_2Cl_2-hexane (1 : 1, *v*/*v*) as eluent to remove any remaining starting material. The product was isolated from the plug using CH_2Cl_2-hexane (1 : 1, *v*/*v*) + 2% MeOH for elution. The solvents were removed *in vacuo* and the residue was recrystallized from CH_2Cl_2-MeOH to give a purple crystalline solid (132 mg, 0.163 mmol, 70%). M.p. = 198–200 °C. – R_f (CH_2Cl_2-hexanes 1 : 1, *v*/*v* + 1% MeOH) = 0.70. – ^{1}H NMR (400 MHz, $CDCl_3$): δ = – 3.07 (br. s, 2H, porphyrin-N*H*), 5.93 (br. s, 1H, N*H*), 5.97 (br. s, 1H, N*H*), 7.15–7.20 (m, 3H, aryl-*H*), 7.47 (t, *J* = 7.4 Hz, 1H, aryl-*H*), 7.72–7.82 (m, 7H, aryl/Ph-*H*), 8.04 (d, *J* = 7.4 Hz, 1H, aryl-*H*), 8.15–8.20 (m, 4H, Ph-*H*), 8.34 (d, *J* = 8.3 Hz, 1H, aryl-*H*), 8.72–8.77 (m, 2H, *β-H*), 8.90 (d, *J* = 4.3 Hz, 2H, *β-H*), 9.03 (d, *J* = 4.3 Hz, 2H, *β-H*), 9.35 (d, *J* = 4.3 Hz, 2H, *β-H*), 10.27 ppm (s, 1H, meso-*H*). – ^{13}C NMR (100 MHz, $CDCl_3$): δ = 105.8, 113.6, 115.3, 117.6, 118.8, 120.0, 120.2, 121.5, 122.0, 124.2, 126.9, 127.0, 129.6, 130.7, 131.1, 131.3, 131.4, 131.8,

132.1, 133.9, 134.6, 134.7, 138.9, 139. 7, 141.0, 145.8, 147.2, 151.6 ppm. – ^{19}F (376 MHz, $CDCl_3$): δ = –63.3 ppm. – UV/Vis (CH_2Cl_2): λ_{max} (lg ε) = 412 (5.50), 510 (4.14), 544 (3.41), 582 (3.62), 638 nm (3.00). – HRMS (MALDI): *m*/*z* = 808.2421 (calcd. 808.2385 for $C_{47}H_{30}F_6N_6O$).

*1-(3,5-Bis(trifluoromethyl)phenyl)-3-(2-[5,15-diphenylporphyrinato-10-yl]zinc(II)-phenyl)urea (**7b**)*

1-(3,5-Bis(trifluoromethyl)phenyl)-3-(2-(5,15-diphenylporphyrin-5-yl)phenyl)urea (120 mg, 0.148 mmol) was dissolved in $CHCl_3$ (30 mL) in a 100 mL round-bottom flask (RBF) and heated to 70 °C. $Zn(OAc)_2{\cdot}2H_2O$ (163 mg, 0.742 mmol) dissolved in MeOH (1 mL) was added to the solution and the reaction was stirred at 70 °C for 1 h. Upon completion, the solvents were removed *in vacuo* and the pink residue was redissolved in CH_2Cl_2-hexanes (1 : 1, *v*/*v*). This solution was filtered through a short plug of silica using CH_2Cl_2-hexanes (1 : 1, *v*/*v*) + 1% MeOH as eluent. The solvents were removed *in vacuo* and the pink residue was recrystallized from CH_2Cl_2-*n*-hexane to give a dark pink solid. Yield based on initial recrystallization (110 mg, 0.126 mmol, 85%). M. p. = 222–225 °C. – R_f (CH_2Cl_2-hexanes 1 : 1, *v*/*v* + 1% MeOH) = 0.52. – ^{1}H NMR (400 MHz, $CDCl_3$-pyridine-d_5, 50 : 1, *v*/*v*): δ = 7.16 (s, 1H, aryl-*H*), 7.25 (app. s, 2H, aryl-*H*), 7.36 (t, *J* = 7.2 Hz, 1H, aryl-*H*), 7.73–7.85 (m, 8H, aryl/Ph-*H*), 8.20–8.29 (m, 4H, Ph-*H*), 8.79 (d, *J* = 4.5 Hz, 2H, *β*-*H*), 8.84 (s, 1H, N-*H*), 8.86 (d, *J* = 4.5 Hz, 2H, *β*-*H*), 9.07 (d, *J* = 4.5 Hz, 2H, *β*-*H*), 9.25 (br. s, 1H, N-*H*), 9.40 (d, *J* = 4.3 Hz, 2H, *β*-*H*), 10.23 ppm (s, 1H, meso-*H*). – ^{13}C NMR (150 MHz, $CDCl_3$-pyridine-d_5, 50 : 1, *v*/*v*): δ = 106.0, 114.0, 117.4, 119.3, 120.2, 121.0, 122.1, 126.4, 126.6, 127.4, 129.1, 130.7, 131.6, 132.2, 132.3, 134.5, 134.8, 134.9, 139.4, 141.0, 143.0, 149.2, 149.6, 150.0, 150.1, 152.8 ppm. – ^{19}F (376 MHz, $CDCl_3$-pyridine-d_5, 50 : 1, *v*/*v*): δ = –63.4 ppm. – UV/Vis (CH_2Cl_2): λ_{max} (log ε) = 414 (5.44), 542 nm (3.97). – HRMS (MALDI): *m*/*z* = 870.1498 (calcd. 870.1520 for $C_{47}H_{28}F_6N_6OZn$).

*1-Phenyl-3-(2-(10,15,20-triphenylporphyrin-5-yl)phenyl)urea (**7c**)*

5-(2-Aminophenyl)-10,15,20-triphenylporphyrin (125 mg, 0.198 mmol) was dried under vacuum for 20 min in a 50 mL Schlenk flask. Anhydrous CH_2Cl_2 (25 mL) was added to dissolve the porphyrin. Phenyl isocyanate (0.03 mL, 0.297 mmol) was added and the solution was left to stir at room temperature for 2 h. TLC analysis showed the presence of starting material, and thus more phenyl isocyanate (0.06 mL, 0.594 mmol) was added. The reaction was left to stir at room temperature for another hour. The solvents were removed *in vacuo* and the residue was redissolved in CH_2Cl_2-hexanes (1 : 1, *v*/*v*) and filtered through a short plug of silica using CH_2Cl_2-hexanes (1 : 1, *v*/*v*) as eluent to remove any remaining starting material. The product was isolated from the plug using CH_2Cl_2+2% MeOH (dark purple band). The solvents were removed *in vacuo* and the residue was recrystallized from CH_2Cl_2-MeOH to give a pink/purple solid (98 mg, 0.131 mmol, 66%). M. p. = 251 °C. – R_f (CH_2Cl_2-hexanes 1 : 1, *v*/*v* + 1% MeOH) = 0.37. – ^{1}H NMR (400 MHz, $CDCl_3$): δ = –2.87 (s, 2H, porphyrin-N*H*), 5.38 (br. s, 1H, urea-N*H*), 5.59 (m, 1H, aryl-*H*), 5.79 (m, 2H, aryl-*H*), 6.04 (br. s, 1H, urea-N*H*), 6.09 (s, 1H, aryl-*H*), 7.43 (t, *J* = 8.3 Hz, 1H, aryl-*H*), 7.71–7.80 (m, 10H, Ph-*H*), 8.00 (d, *J* = 7.5 Hz, 1H, aryl-*H*), 8.15–8.21 (m, 6H, Ph-*H*), 8.52 (d, *J* = 7.5 Hz, 1H, aryl-*H*), 8.70 (d, *J* = 4.3 Hz, 2H, *β*-*H*), 8.80 (d, *J* = 4.3 Hz, 2H, *β*-*H*), 8.85 ppm (s, 4H, *β*-*H*). – ^{13}C NMR (100 MHz, $CDCl_3$): δ = 113.2, 119.8, 120.0, 120.1, 120.4, 121.0, 121.7, 122.9, 126.8, 127.8, 127.9, 129.6, 130.8, 134.0, 134.5, 134.6, 136.4, 139.4, 141.7, 141.9, 152.3 ppm. – HRMS (MALDI): *m*/*z* = 748.2955 (calcd. 748.2951 for $C_{51}H_{36}N_6O$).

*1-Phenyl-3-(2-[10,15,20-triphenylporphyrinato-5-yl]zinc(II)-phenyl)urea (**7d**)*

[5-(2-Aminophenyl)-10,15,20-triphenylporphyrinato]zinc(II) (150 mg, 0.216 mmol) was dried under vacuum for 20 min in a 100 mL Schlenk flask. Anhydrous CH_2Cl_2 (30 mL) was added to dissolve the porphyrin. Phenyl isocyanate (0.04 mL, 0.325 mmol) was added and the solution

was stirred at room temperature for 2 h. TLC analysis showed the presence of starting material, and thus more phenyl isocyanate (0.05 mL, 0.406 mmol) was added. The mixtion was stirred at room temperature for another hour. The solvents were removed *in vacuo* and the residue was redissolved in CH_2Cl_2 and filtered through a short plug of silica using CH_2Cl_2 as eluent to remove any remaining starting material. The product was isolated from the plug using CH_2Cl_2+1% MeOH (dark purple band). The solvents were removed *in vacuo* and the residue was recrystallized from CH_2Cl_2-*n*-hexane to give a pink solid (130 mg, 0.160 mmol, 74%). M. p. = 249–251 °C. – R_f (CH_2Cl_2-hexanes 1 : 1, *v*/*v*) = 0.31. – ^{1}H NMR (400 MHz, $CDCl_3$): δ = 6.27 (s, 1H, N*H*), 6.44–6.53 (m, 4H, aryl-*H*), 6.94 (s, 1H, aryl-*H*), 7.32 (t, *J* = 7.6 Hz, 1H, aryl-*H*), 7.63 (s, 1H, N*H*), 7.65–7.76 (m, 1H, Ph/aryl-*H*), 7.82 (d, *J* = 7.6 Hz, 1H, aryl-*H*), 8.10-8.26 (m, 6H, Ph-*H*), 8.73 (d, *J* = 4.7 Hz, 2H, *β*-*H*), 8.77 (d, *J* = 4.7 Hz, 2H, *β*-*H*), 8.84–8.87 ppm (m, 4H, *β*-*H*). – ^{13}C NMR (100 MHz, $CDCl_3$-pyridine-d_5): δ = 114.0, 118.9, 119.3, 120.6, 120.7, 121.2, 121.9, 126.3, 126.4, 126.5, 127.3, 128.2, 129.0, 130.8, 131.6, 131.7, 132.3, 134.4, 134.5, 134.6, 134.7, 139.9, 143.2, 143.3, 149.7, 150.0, 153.2 ppm. – UV/Vis (CH_2Cl_2): λ_{max} (log ε) = 420 (5.75), 546 (4.30), 586 nm (3.27) nm. – HRMS (MALDI): *m*/*z* = 810.2102 (calcd. 810.2086 for $C_{51}H_{34}N_6OZn$).

*1-(3,5-Bis(trifluoromethyl)phenyl)-3-(2-[10,15,20-triphenylporphyrinato-5-yl]zinc(II)-phenyl)urea (**7e**)*

[5-(2-Aminophenyl)-10,15,20-triphenylporphyrinato]zinc(II) (100 mg, 0.144 mmol) was dried under vacuum for 20 min in a 100 mL Schlenk flask. Anhydrous CH_2Cl_2 (25 mL) was added to dissolve the porphyrin. (3,5-Bistrifluoromethyl)phenyl isocyanate (0.01 mL, 0.325 mmol) was added and the mixture was stirred at room temperature for 18 h. The solvents were removed *in vacuo* and the residue was redissolved in CH_2Cl_2 and filtered through a short plug of silica using CH_2Cl_2 as eluent to remove any remaining starting material. The product was isolated

from the plug using CH_2Cl_2+2% MeOH (dark purple band). The solvents were removed *in vacuo* and the residue was recrystallized from CH_2Cl_2-*n*-hexane to give a purple solid (82 mg, 0.087 mmol, 60%). M. p. = 256 °C. – R_f (CH_2Cl_2-hexanes 1 : 1, *v*/*v* + 1% MeOH) = 0.33. – ^{1}H NMR (400 MHz, $CDCl_3$-pyridine-d_5): δ = 7.13 (s, 1H, N*H*), 7.26 (s, 1H, aryl-*H*), 7.32 (t, *J* = 7.5 Hz, 1H, aryl-*H*), 7.66–7.78 (m, 13H, aryl/Ph-*H*), 8.11–8.22 (m, 6H, Ph-*H*), 8.26 (s, 1H, aryl-*H*), 8.71–8.73 (m, 2H, *β*-*H*), 8.76–8.78 (m, 2H, *β*-*H*), 8.81 (d, *J* = 7.5 Hz, 1H, aryl-*H*), 8.85–8.88 (m, 4H, *β*-*H*), 9.21 ppm (s, 1H, N*H*). – ^{13}C NMR (100 MHz, $CDCl_3$-pyridine-d_5): δ = 113.4, 114.6, 117.3, 119.2, 120.7, 120.9, 126.3, 126.4, 127.3, 129.1, 130.6, 131.6, 131.7, 132.2, 134.3, 134.7, 134.8, 139.4, 141.1, 143.1, 143.3, 149.5, 149.7, 152.8 ppm. – ^{19}F (376 MHz, $CDCl_3$-pyridine-d_5): δ = –63.4 ppm. – UV/Vis (CH_2Cl_2): λ_{max} (log ε) = 422 (5.65), 548 (4.27), 590 nm (3.33). – HRMS (MALDI): *m*/*z* = 946.1862 (calcd. 946.1833 for $C_{53}H_{32}F_6N_6OZn$).

*2-((10,15,20-Triphenylporphyrin-5-yl)ethynyl)aniline (**9a**)*

5-Bromo-10,15,20-triphenylporphyrin (300 mg, 0.486 mmol) was added to a 100 mL Schlenk tube and dried under vacuum for 15 min. Anhydrous THF (15 mL) and triethylamine (5 mL) were added and the solution was degassed *via* 3 freeze-pump-thaw cycles. CuI (19 mg, 0.097 mmol), $PdCl_2(PPh_3)_2$ (51 mg, 0.073 mmol) and 2-ethynylaniline (0.6 g in 2 mL anhydrous THF, 5.106 mmol) were added under argon and the reaction mixture was heated to 40 °C and stirred at this temperature for 24 h. Upon completion, the solvents were removed *in vacuo* and the residue was redissolved in CH_2Cl_2 and washed with sat. aqueous $NaHCO_3$ solution, brine, and H_2O using CH_2Cl_2 to extract the product. The organic extracts were combined and dried over Na_2SO_4. Following filtration, the solvents were removed *in vacuo* and the residue was redissolved in CH_2Cl_2-hexane (1 : 2, *v*/*v*) to remove the Cu(II) insertion side-product. Using CH_2Cl_2 as eluent, the product was isolated as the second fraction. The solvents were removed

in vacuo and the residue was recrystallized from CH_2Cl_2-MeOH to give a green/purple solid (230 mg, 72%, 0.352 mmol). M. p. = 294–296 °C. – R_f (CH_2Cl_2-hexane-MeOH 1 : 1 : 0.05, *v*/*v*/*v*) = 0.63. – ^{1}H NMR (400 MHz, $CDCl_3$): δ = –2.31 (br. s, 2H, N*H*), 4.66 (br. s, 2H, N*H*), 6.88–6.94 (m, 2H, aniline-*H*), 7.29 (t, *J* = 7.3 Hz, 1H, aniline-*H*), 7.75–7.80 (m, 9H, Ph-*H*), 7.83 (d, *J* = 7.3 Hz, aniline-*H*), 8.16–8.22 (m, 6H, Ph-*H*), 8.76 (app. s, 4H, *β*-*H*), 8.89 (d, *J* = 4.2 Hz, 1H, aryl-*H*), 8.85–8.88 (m, 4H, *β*-*H*), 9.21 ppm (s, 1H, N*H*). – ^{13}C NMR (100 MHz, $CDCl_3$): δ = 93.4, 97.1, 99.6, 108.8, 114.7, 118.3, 121.1, 121.8, 126.7, 126.8, 127.8, 130.1, 132.3, 134.4, 134.5, 141.7, 141.9, 148.5 ppm. – UV/Vis (CH_2Cl_2): λ_{max} (log ε) = 434 (5.50), 534 (4.12), 579 (4.51), 670 nm (4.13). – HRMS (MALDI): *m*/*z* = 653.2578 (calcd. 653.2579 for $C_{46}H_{31}N_5$).

*2-([10,15,20-Triphenylporphyrinato-5-yl]zinc(II)-ethynyl)aniline (**9b**)*

[5-Bromo-10,15,20-triphenylporphyrinato]zinc(II) (100 mg, 0.147 mmol) was added to a 100 mL Schlenk tube and dried under vacuum for 15 min. Anhydrous DMF (8 mL) and diethylamine (3 mL) were added and the solution was degassed *via* 3 freeze-pump-thaw cycles. CuI (6 mg, 0.029 mmol), $PdCl_2(PPh_3)_2$ (16 mg, 0.022 mmol) and crude 2-ethynylaniline (0.1 g in DMF solution) were added under argon and the reaction mixture was heated to 120 °C and stirred at this temperature for 18 h. Upon completion, the solvents were removed *in vacuo* and the residue was redissolved in CH_2Cl_2 and filtered through a plug of silica using CH_2Cl_2 as eluent to removed traces of starting material and using CH_2Cl_2 + 1% MeOH to remove the product (bright green fraction). The solvents were removed *in vacuo* and the residue was recrystallized from CH_2Cl_2-*n*-hexane to give a green/purple solid (73 mg, 70%, 0.101 mmol). M. p. = >300 °C. – R_f (CH_2Cl_2-hexane 1 : 1, *v*/*v*) = 0.39. ^{1}H NMR (400 MHz, $CDCl_3$-pyridine-d_5): δ = 4.72 (br. s, 2H, N-H_2), 6.90 (app. d, *J* = 7.3 Hz, 2H, aryl-*H*), 7.64–7.72 (m, 10H, Ph/aryl-*H*), 7.82 (d, *J* = 7.3 Hz, 1H, aryl-*H*), 8.10–8.17 (m, 6H, Ph-*H*), 8.75 (br. s, 4H, *β*-*H*), 8.89 (d, *J*

= 3.9 Hz, *β-H*), 9.72 ppm (d, *J* = 3.9 Hz, 2H, *β-H*). – ^{13}C NMR (100 MHz, $CDCl_3$-pyridine-d_5): δ = 98.7, 114.6, 118.2, 121.6, 126.3, 126.4, 127.2, 129.6, 130.5, 132.6, 134.4, 134.5, 142.4, 143.1, 148.4, 148.9, 149.2, 150.4, 152.0 ppm. – UV/Vis (CH_2Cl_2): λ_{max} (lg ε) = 434 (5.32) 560 (4.08), 605 nm (4.12). – HRMS (MALDI): *m*/*z* = 715.1746 (calcd. 715.1714 for $C_{46}H_{29}N_5Zn$).

*1-(3,5-Bis(trifluoromethyl)phenyl)-3-(2-((10,15,20-triphenylporphyrin-5-yl)ethynyl)phenyl)urea (**10a**)*

2-((10,15,20-Triphenylporphyrin-5-yl)ethynyl)aniline (200 mg, 0.306 mmol) was dried under vacuum for 20 min in a 100 mL Schlenk flask. Anhydrous CH_2Cl_2 (25 mL) was added to dissolve the porphyrin. 3,5-Bistrifluoromethylphenyl isocyanate (0.11 mL, 0.612 mmol) was added and the reaction mixture was stirred at room temperature for 2 h, diluted with CH_2Cl_2 and washed with H_2O (50 mL × 3). The organic extracts were dried over Na_2SO_4 and filtered. The solvents were removed *in vacuo* and the residue was recrystallized from CH_2Cl_2-MeOH to give a crystalline purple solid (210 mg, 0.230 mmol, 76%). M. p. = 298–300 °C. – R_f (CH_2Cl_2-hexane-MeOH 1 : 1 : 0.05, *v*/*v*/*v*) = 0.51. – ^{1}H NMR (400 MHz, $CDCl_3$-pyridine-d_5, 30 : 1): δ = –2.51 (br. s, 1H, N-*H*), 7.18 (t, *J* = 7.1 Hz, 1H, aryl-*H*), 7.38 (s, 1H, aryl-*H*), 7.46 (t, *J* = 7.1 Hz, 1H, aryl-*H*), 7.68–7.75 (m, 9H, Ph-*H*), 7.82 (s, 2H, aryl-*H*), 7.87 (d, *J* = 7.4 Hz, 1H, aryl-*H*), 8.14 (d, *J* = 7.2 Hz, 6H, Ph-*H*), 8.33 (br. s, 1H, N-*H*), 8.41 (d, *J* = 8.1 Hz, 1H, aryl-*H*), 8.77–8.82 (m, 6H, *β-H*), 9.46 (d, *J* = 4.6 Hz, 2H, *β-H*), 10.31 ppm (br. s, 1H, N-*H*). – ^{13}C NMR (100 MHz, $CDCl_3$-pyridine-d_5, 30 : 1): δ = 91.2, 97.5, 98.0, 112.8, 115.3, 118.2, 119.9, 121.3, 121.8, 122.4, 126.8, 126.9, 127.9, 130.1, 131.7, 132.1, 132.5, 134.3, 134.4, 140.4, 141.4, 141.7, 152.9 ppm. – ^{19}F NMR (376 MHz, $CDCl_3$-pyridine-d_5, 30 : 1): δ = –63.18 ppm. – UV/Vis (CH_2Cl_2): λ_{max} (lg ε) = 432 (5.38), 530 (3.88), 574 (4.19), 608 (3.66), 667 nm (3.88). – HRMS (MALDI): *m*/*z* = 908.2715 (calcd. 908.2698 for $C_{55}H_{34}N_6OF_6$).

*1-(3,5-Bis(trifluoromethyl)phenyl)-3-(2-([10,15,20-triphenylporphyrinato-5-yl]zinc(II))ethynyl)phenyl)urea (**10b**)*

1-(3,5-Bis(trifluoromethyl)phenyl)-3-(2-((10,15,20-triphenylporphyrin-5-yl)ethynyl)phenyl)urea (200 mg, 0.220 mmol) was dissolved in $CHCl_3$ (25 mL) in a 100 mL RBF and heated to 70 °C. $Zn(OAc)_2 \cdot 2H_2O$ (200 mg, 0.909 mmol) dissolved in MeOH (1 mL) was added and the reaction mixture was stirred at 70 °C for 1 h. Upon complete consumption of starting material the solvents were removed *in vacuo* and the residue was redissolved in CH_2Cl_2 and washed with sat. aqueous $NaHCO_3$ solution (3 × 25 mL) and H_2O (3 × 25 mL). The organic extracts were dried over Na_2SO_4 and filtered, and the solvents were removed. The residue was recrystallized from CH_2Cl_2-*n*-hexane to give a fine green solid (110 mg, 51%, 0.113 mmol). The mother liquor was concentrated *in vacuo* to give a green solid which showed similar analytical data to that of the recrystallized solid (80 mg, 37%, 0.082 mmol). Total yield (190 mg, 88%, 0.195 mmol). M. p. >300 °C. – R_f (CH_2Cl_2-hexane-MeOH 1 : 1 : 0.05, *v*/*v*/*v*) = 0.29. – ^{1}H NMR (400 MHz, $CDCl_3$-pyridine-d_5, 30 : 1): δ = 7.18 (t, *J* = 7.1 Hz, 1H, aryl-*H*), 7.38 (s, 1H, aryl-*H*), 7.46 (t, *J* = 7.1 Hz, 1H, aryl-*H*), 7.68–7.75 (m, 9H, Ph-*H*), 7.82 (s, 2H, aryl-*H*), 7.87 (d, *J* = 7.4 Hz, 1H, aryl-*H*), 8.14 (d, *J* = 7.2 Hz, 6H, Ph-*H*), 8.33 (br. s, 1H, N-*H*), 8.41 (d, *J* = 8.1 Hz, 1H, aryl-*H*), 8.77–8.82 (m, 6H, *β*-*H*), 9.46 (d, *J* = 4.6 Hz, 2H, *β*-*H*), 10.31 ppm (br. s, 1H, N-*H*). – ^{13}C NMR (100 MHz, $CDCl_3$-pyridine-d_5): δ = 89.9, 97.5, 99.4, 113.5, 115.4, 118.3, 119.8, 121.8, 122.9, 123.1, 124.5, 126.4, 126.5, 127.4, 129.6, 130.4, 131.7, 132.2, 134.3, 134.4, 140.0, 141.3, 142.8, 142.9, 149.6, 149.8, 150.6, 152.0, 152.8 ppm. – ^{19}F NMR (376 MHz, $CDCl_3$-pyridine-d_5, 30 : 1): δ = –63.15 ppm. – UV/Vis (CH_2Cl_2): λ_{max} (lg ε) = 436 (5.43) 562 (4.10), 608 nm (4.16). – HRMS (MALDI): *m*/*z* = 970.1847 (calcd. 970.1833 for $C_{55}H_{32}N_6OF_6Zn$).

X-ray structure determination

Crystals were grown using techniques following the protocol developed by Hope [23, 24] (liquid-liquid diffusion in CH_2Cl_2 and methanol). The crystal was mounted on a MiTeGen MicroMount and single-crystal X-ray diffraction data were collected on a Bruker APEX 2 DUO CCD diffractometer using graphite-monochromated Mo$K\alpha$ (λ = 0.71073 Å) radiation at T = 100(2) K with an Oxford Cryosystems Cobra low-temperature device. Data was collected by using ω and φ scans and corrected for Lorentz and polarization effects by using the APEX software suite [25–27]. Using OLEX2, the structure was solved with the XS structure solution program, using Direct Methods and refined against $|F^2|$ with XL using least-squares minimization [28]. The C- and N-bound H atoms were placed in their expected calculated positions and refined as riding model: N–H = 0.88 Å, C–H = 0.95–0.98 Å, with U_{iso} (H) = 1.5U_{eq} (C) for methyl H atoms and 1.2U_{eq} (C, N) for all other H atoms. Details of data refinements can be found in Table 1. All images were prepared by using OLEX2 [27]. The structure was refined as an inversion twin. There is a large residual of 2.21 e Å^{-3} which is 0.82 Å from Zn1. The solvent molecule (CH_2Cl_2) was disordered over 3 sites with refined occupancies of 80, 10, and 10%. Geometrical restraints were applied. The solution of P1 was chosen as the optimal over other solutions such as $P\bar{1}$ which has an 80% fit as determined by ADDSYM. When modeling in $P\bar{1}$, the structure is improbable as both the urea moiety and the axial methanol ligand occupying the same position. As a result, much higher R values, poor GOOF, high residual density, and significant disorder on the porphyrin macrocycle which would need to be extensively modeled beyond any reasonable expectation of accuracy. This modeling would result in a structure similar to that of the P1 solution which does not require such treatments.

CCDC 2007941 contains the supplementary crystallographic data for this paper. These data can be obtained free of charge from The Cambridge Crystallographic Data Centre *via* www.ccdc.cam.ac.uk/data_request/cif.

Acknowledgment: This work was supported by a grants from Science Foundation Ireland (SFI, IvP 13/IA/1894) and through funding from the European Union's Horizon 2020 research and innovation program under the FET Open grant agreement no. 828779.

[1] Gotico P., Boitrel B., Guillot R., Sircoglou M., Quaranta A., Halime Z., Leibl W., Aukauloo A. *Angew. Chem. Int. Ed*. 2019, *58*, 4504–4509.

[2] Ladomenou K., Bonar-Law R. P. *Chem. Commun.* 2002, 2108–2109.

[3] Uddin S. M. N., Nagao Y. *Langmuir* 2017, *33*, 12777–12784.

[4] Calderon-Kawasaki K., Kularatne S., Li Y. H., Noll B. C., Scheidt W. R., Burns, D. H. *J. Org. Chem.* 2007, *72*, 9081–9087.

[5] Norvaiša K., Flanagan K. J., Gibbons D., Senge M. O. *Angew. Chem. Int. Ed*. 2019, *58*, 16553–16557.

[6] Kielmann M., Senge M. O. *Angew. Chem. Int. Ed*. 2018, *58*, 418–441.

[7] Roucan M., Kielmann M., Connon S. J., Bernhard S. S. R., Senge M. O. *Chem. Commun.* 2018, *54*, 26–29.

[8] Simonneaux G., Srour H., Le Maux P., Chevance S., Carrie D. *Symmetry* 2014, *6*, 210–221.

[9] Callaghan S., Flanagan K. J., O'Brien J. E., Senge M. O. *Eur. J. Org. Chem*. 2020, 2735–2744.

[10] Frost J. R., Huber S. M., Breitenlechner S., Bannwarth C., Bach T. *Angew. Chem. Int. Ed.* 2015, *54*, 691–695.

[11] Burg F., Breitenlechner S., Jandla C., Bach T. *Chem. Sci*. 2020, *11*, 2121–2129.

[12] Hyslop A. G., Kellett M. A., Iovine P. M., Therien M. J. *J. Am. Chem. Soc.* 1998, *120*, 12676–12677.

[13] Yan L., Che X., Bai X., Pei Y. *Mol. Divers.* 2012, *16*, 489–501.

[14] Abraham T., Soloski E. J., Benner C. L., Evers R. C. *J. Polym. Sci., Part A: Polym. Chem.,* 1989, *27,* 4305–4318.

[15] Groom C. R., Bruno I. J., Lightfoot M. P., Ward S. C. *Acta Crystallogr*. 2016, *B72*, 171–179.

[16] Lin W., Cen T.-Y., Wang S.-P., Zhang Z., Wu J., Huang J., Li S. *Chin. Chem. Lett*. 2018, *29*, 1372–1374.

[17] Jagessar R. C., Shang M., Scheidt W. R., Burns D. H. *J. Am. Chem. Soc.* 1998, *120*, 11684–11692.

[18] Hirshfeld F. L. *Theor. Chim. Acta* 1977, *44*, 129–138.

[19] Turner M. J., McKinnon J. J., Wolff S. K., Grimwood D. J., Spackman P. R., Jayatilaka D., Spackman M. A., CrystalExplorer17 2017, University of Western Australia.

[20] Ryan A., Gehrold A., Perusitti R., Pintea M., Fazekas M., Locos O. B., Blaikie F., Senge M. O. *Eur. J. Org. Chem*. 2011, 5817–5844.

[21] Goudriaan P. E., Jang X.-B., Kuil M., Lemmens R., Van Leeuwen P. W. N. M., Reek J. N. H. *Eur. J. Org. Chem*. 2008, 6079–6092.

[22] Collman J. P., Brauman J. I., Doxsee K. M., Halbert T. R., Bumenberg E., Linder R. E., LaMar G. N., Del Gaudio J., Lang G., Spartalian K. *J. Am. Chem. Soc*. 1980, *102*, 4182–4192.

[23] Hope H. *Prog. Inorg. Chem*. 2007, *41*, 1–19.

[24] Senge M. O. *Z. Naturforsch.* 2000, *55b*, 336–344.

[21] SAINT (version 8.37a). Bruker AXS Inc.: Madison, Wisconsin (USA), 2013.

[25] SADABS (version 2016/2). Bruker AXS Inc.: Madison, Wisconsin (USA), 2016.

[26] APEX3 (version 2016.9-0). Bruker AXS Inc.: Madison, Wisconsin (USA), Madison, WI, 2016.

[27] Dolomanov O. V., Bourhis L. J., Gildea R. J., Howard J. A. K., Puschmann H. *J. Appl. Crystallogr*. 2009, *42*, 339–341.

[28] Sheldrick G. *Acta Crystallogr.* 2015, *A71*, 3–8.

Table 1. Crystal structure data for compound **7d·MeOH**.

Empirical formula	$C_{53}H_{40}Cl_2N_6O_2Zn$
Formula weight	929.18
Temperature / K	100.05
Crystal system	triclinic
Space group	*P*1
a / Å	10.6399(4)
b / Å	10.6610(4)
c / Å	11.8052(5)
α / deg	107.605(1)
β / deg	105.636(1)
γ / deg	109.220(1)
Volume / Å^3	1099.22(8)
Z	1
ρ_{calcd} / g cm^{-3}	1.40
μ / mm^{-1}	0.7
F(000), *e*	480
Crystal size / mm^3	0.41 × 0.31 × 0.11
Radiation; λ / Å	Mo*Kα*; 0.71073
2θ range for data collection / deg	3.968–51.000
hkl ranges	±12; ±12; ±14
Reflections collected	17623
Independent reflections	7225
R_{int}; R_{sigma}	0.0152; 0.0317
Data; restraints; parameters	7225; 65; 642
Goodness-of-fit on F^2	1.063
Final R_1; wR_2 [$I \geq 2\,\sigma(I)$]	0.0479; 0.1247
Final R_1; wR_2 (all data)	0.0491; 0.1259
Flack (*x*)	0.099(14)
Res. electron dens. (max; min) / *e* Å^{-3}	2.21/-0.58

Content section suggestions: ok!